NJC

PAPER

View Article Online
View Journal

Cite this: DOI: 10.1039/c6nj00243a

Dendrimeric magnetic nanoparticle cores with Co-phthalocyanine tags and their application in the synthesis of tetrahydrobenzo[*b*]pyran derivatives†

Mohamad Ali Zolfigol,*[a] Maliheh Safaiee*[b] and Neda Bahrami-Nejad[a]

Received (in Montpellier, France) 24th January 2016,
Accepted 18th March 2016

DOI: 10.1039/c6nj00243a

www.rsc.org/njc

A new and rational method for the synthesis of Fe_3O_4@SiO_2@$SiO_2(CH)_3Cl$ based magnetic nanoparticles with amino cobalt phthalocyanine tags (ACoPc-MNPs) was described and these were evaluated as a reusable catalyst for the one-pot synthesis of tetrahydrobenzo[*b*]pyran derivatives. The described reaction proceeded in high to excellent yield, with a short reaction time, and under mild and green solvent-free conditions at room temperature. The ACoPc-MNP catalyst was characterized *via* Fourier transform infrared spectroscopy (FT-IR), X-ray diffraction (XRD), thermal gravimetric analysis (TGA), scanning electron microscopy (SEM), atomic force microscopy (AFM), transmission electron microscopy (TEM), Brunauer–Emmett–Teller (BET), X-ray fluorescence (XRF) analysis, energy-dispersive X-ray spectroscopy (EDX) and vibrating sample magnetometry (VSM). Moreover, the catalyst could be easily recovered by magnetic separation and recycled 4 times without significant loss of its catalytic activity. Moreover, by this synthetic method, some novel tetrahydrobenzo[*b*]pyran derivatives are prepared and characterized.

1. Introduction

The rational design, synthesis and application of magnetically recoverable catalysts has received immense attention as a fascinating choice to enhance the efficiency of heterogeneous nanocatalyst separation from the reaction mixture by simply applying a magnet.[1] On the other hand, rational design of functionalized phthalocyanines (Pcs) allows for the creation of additional functionalities in the magnetic nanoparticles (MNPs) to influence either their physical or chemical properties. The combination of functionalized phthalocyanines (Pcs) and magnetic nanoparticles (MNPs) provides fantastic heterogeneous systems where different bond cleavage and formation processes and various functional group interconversions can be induced by the Pc functionality.

Phthalocyanine (Pc) is an aromatic macrocyclic compound that is widely used as a pigment in textiles, polymers and paints.[2] It presents great structural flexibility and molecular diversity and can host nearly 70 different elements in the central core of its cavity. Therefore, phthalocyanines can be used as catalysts due to their electrical conductivity, excellent thermal stability and extraordinary mechanical properties for oxidation, reduction and synthesis of various organic compounds,[3] in transistors,[4] gas sensors, optical disks, liquid crystals,[5] semiconductors,[6] non-linear optics[7] and as photosensitizers in photodynamic therapy (PDT)[8] for cancer. Among metallophthalocyanines, cobalt phthalocyanine is known to display the ability to promote the $4e^-$ oxygen reduction to water.[9]

These compounds are synthesized by reaction between metal salts, urea and phthalonitriles, phthalic anhydride[10] or phthalimide.

Typically, temperatures around 200 °C and reaction times of several hours are needed for such reactions.[11]

Recently, magnetite nanoparticles (MNPs) have offered advantages in the development of clean and sustainable supports as they have a large surface area and are non-toxic, readily accessible, and retrievable. Among magnetic nanoparticles (MNPs), nano-magnetic core–shell structures are extensively applied in biological and environmental research studies. The magnetic core–shell, consisting of an iron oxide core and a silica shell, has attracted much attention for its unique magnetic properties, low cyto-toxicity, good stability, and chemically modifiable surface.[12]

Thus, immobilization of Co phthalocyanine (Co-Pc) *via* covalent attachment to the surface of the magnetic core–shell is an interesting method to facilitate catalyst recovery and recycling and reduce sewage pollution.[13]

Multicomponent reactions (MCRs) are those reactions in which three or more reactants react simultaneously to provide

[a] Department of Organic Chemistry, Faculty of Chemistry, Bu-Ali Sina University, Hamedan 6517838683, Iran. E-mail: zolfi@basu.ac.ir, mzolfigol@yahoo.com; Fax: +988138380709; Tel: +988138282807

[b] Department of Medicinal Plants Production, Nahavand University, Nahavand, 6593139565, Iran. E-mail: azalia_s@yahoo.com, msafaiee@nahgu.ac.ir

† Electronic supplementary information (ESI) available. See DOI: 10.1039/c6nj00243a

the product in a single step under appropriate reaction conditions. A large variety of MCRs, particularly three-component coupling reactions, are performed in the presence of acid catalysts.[14]

MCRs leading to heterocyclic scaffolds are particularly useful for the creation of drug-like molecules. One prominent MCR that produces an interesting class of oxygen heterocyclic compounds is tetrahydrobenzo[*b*]pyran synthesis.

4*H*-Benzo[*b*]pyran and its derivatives have useful biological and pharmacological properties, such as spasmolytic, anticoagulant, diuretic, anticancer, and antianaphylactin characteristics.[15]

With this aim, we decided to design and synthesize novel nanomagnetically separable systems in which Co phthalocyanine is chemically anchored to the nanomagnetite core–shell and apply them in the synthesis of tetrahydrobenzo[*b*]pyran derivatives. The results show that the thus obtained magnetically heterogeneous nanocatalysts are useful for the synthesis of the described compounds without having the inherent limitation of leaching.

2. Results and discussion

2.1. Catalyst synthesis and characterization

Development of task-specific magnetic nanoparticle (MNP) catalysts and their structural diversity could be achieved *via* design and synthesis of novel core–shells with suitable phthalocyanine tags. By considering the above-mentioned synthetic strategy, in the course of a decade of investigation on design and synthesis of solid acids,[16] MNP catalysts[17] and phthalocyanine,[18] we are able to report novel ACoPc-MNPs. With this aim, we decided to design and synthesize a basic ACoPc-MNP (Schemes 1 and 2). Thus, ACoPc-MNPs were synthesized and fully characterized by Fourier transform infrared spectroscopy (FT-IR), X-ray diffraction (XRD), thermal gravimetric analysis (TGA), scanning electron microscopy (SEM), atomic force microscopy (AFM), transmission electron microscopy (TEM), Brunauer–Emmett–Teller (BET), X-ray fluorescence (XRF) analysis, energy-dispersive X-ray spectroscopy (EDX) and vibrating sample magnetometry (VSM). In this work the ACoPc-MNPs were synthesized by using two methods:

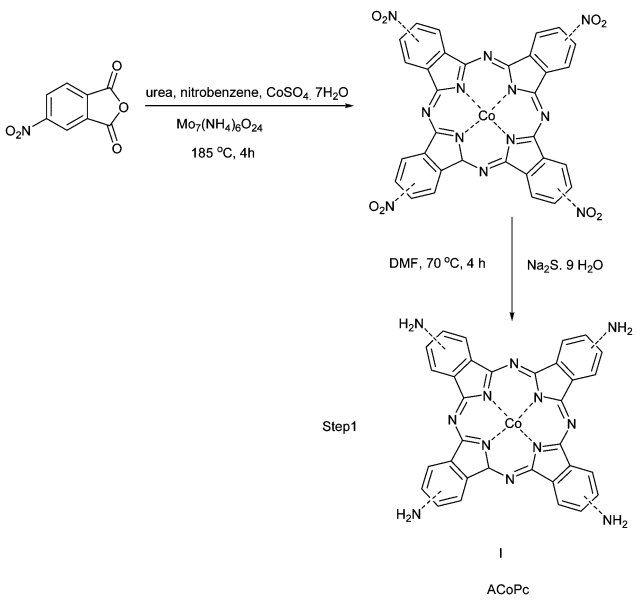

Scheme 1 Synthesis of ACoPc (I).

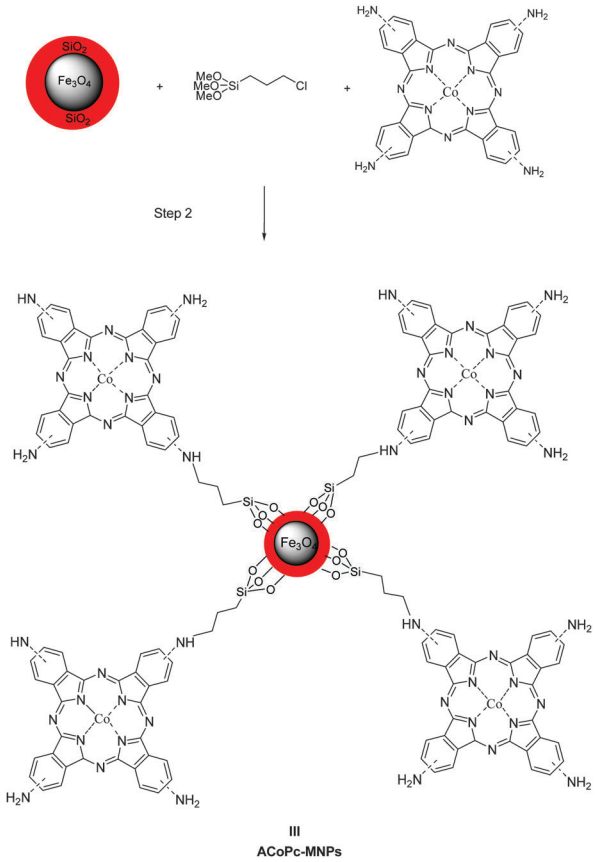

Scheme 2 Synthesis of ACoPc-MNPs by method 1.

Method 1. To prepare the catalyst, nitro Co phthalocyanine (NCoPc) was prepared according to our previously reported procedure.[18] After that, reduction of nitro to amino groups was done by using sodium sulfide nonahydrate (Scheme 1). The amino Co phthalocyanine (ACoPc) was characterised using UV-visible spectroscopy.

The UV-visible spectrum of amino Co phthalocyanine (ACoPc) complexes in freshly distilled DMF is shown in Fig. 1. The UV-visible spectrum confirmed the creation of ACoPc. The UV-visible spectrum consists of three absorption bands in fresh DMF. In the region of 767 nm the Q band was observed. It was shifted out of the visible region into the near infrared region so that the color of the synthesized complex was dark green.[19] The large red shift of the Q band is due to the large electron-donating ability of the amino groups. The weaker band in the region of 328 nm is called B or the Soret band and finally charge transfer transitions are located between Q and B bands. A broad band between 400 and 540 is probably due to charge transfer.

FT-IR spectroscopy indicated the successful synthesis of ACoPc. The peaks at 1615 and 1434 cm^{-1} are assigned to C═N and C═C of phthalocyanine, respectively. The other

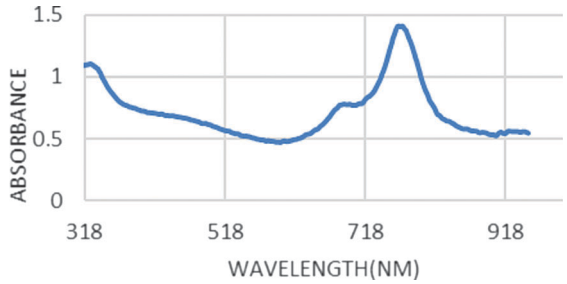

Fig. 1 UV-vis spectrum of ACoPc in DMF.

absorption peak at 3442 could be assigned to NH_2 stretching due to the presence of an amino functional group in ACoPc.

Then, ACoPc reacted with the Fe_3O_4@SiO_2 core–shell and (3-chloropropyl)trimethoxysilane [CPTMS] under refluxing conditions to give ACoPc-MNPs (Scheme 2). Subsequently, the synthesized catalyst was fully characterized by FT-IR, XRD, XRF, SEM, TEM, AFM, TGA, VSM, BET and elemental analysis.

The other method was also suggested to find the best way for the synthesis of the catalyst which is indicated in Scheme 2.

Method 2. Fe_3O_4 coated silica reacts with CPTMS to produce chloro-functionalized MNPs, Fe_3O_4@SiO_2@$SiO_2(CH_2)_3Cl$ [ClMNPs] (Scheme 3). Then, to covalently link the ClMNPs to ACoPc, chloro-functionalized MNPs and toluene were sonicated and subsequently added to the ACoPc.

Step by step formation of the support was confirmed by using FT-IR. The Fourier transform spectra of (a) Fe_3O_4@SiO_2, (b) Fe_3O_4, and (c) Fe_3O_4@SiO_2@$SiO_2(CH_2)_3Cl$ modified by CPTMS are shown in Fig. 2. In Fig. 2b, the band at 592 cm^{-1} is related to the Fe–O bending vibration. The silica coating of magnetite nanoparticles was confirmed by the observation of a high-intensity band at about 1098 cm^{-1} assigned to asymmetric stretching bonds of Si–O–Si in SiO_2. The broad peaks in the range 3100–3600 cm^{-1} and the weak peak at 1632 cm^{-1} are assigned to the O–H stretching vibration mode (Si–OH) and surface hydroxyl groups or adsorbed water on the sample surface, respectively. The broad band with a low intensity in the 2750–3000 cm^{-1} region is allocated to C–H stretching of methylene groups (Fig. 2c). Thus, the above results indicate that the chloro functional groups were successfully grafted onto the surface of the magnetic Fe_3O_4@SiO_2 nanoparticles.[20]

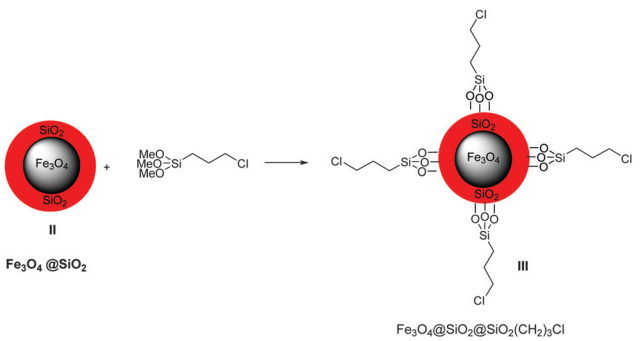

Scheme 3 Synthesis of chloro-functionalized MNPs for synthesis of ACoPc-MNPs by method 2.

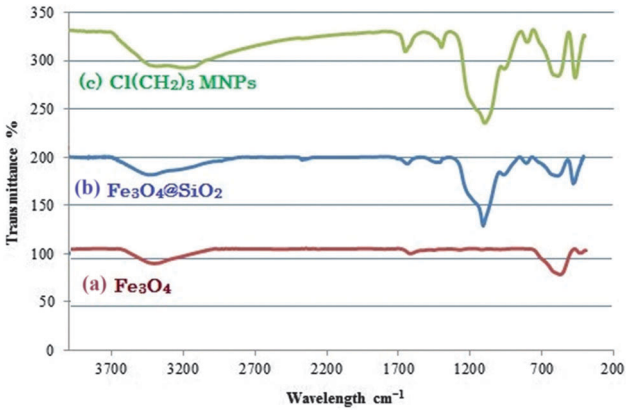

Fig. 2 FT-IR spectra of the supporting production process of (a) Fe_3O_4, (b) Fe_3O_4@SiO_2, and (c) $Cl(CH_2)_3$MNPs.

Immobilization of the ACoPc on MNPs was confirmed by FT-IR spectroscopy as indicated in Fig. 3. ACoPc-MNPs had several absorption peaks at around 1617, 1438 and 1101, which could be assigned to phthalocyanine skeletal and SiO_2 vibrations. The results revealed that ACoPc was successfully coated onto the surface of Fe_3O_4@SiO_2 nanoparticles.

In conclusion, comparison of the two methods revealed them to be the same, as indicated by the IR spectra. So, the two methods can be used to make the catalysts (Fig. 4).

Another indication of bond formation between Co phthalocyanine and the support can be inferred from TGA. TGA of the synthesized catalyst shows two steps of weight loss and indicates the presence of supported organic functional groups. The initial mass loss below 200 °C is the result of the removal of physically adsorbed solvent and surface hydroxyl groups. The mass loss of about 84% between 200 °C and nearly 555 °C is attributed to the thermal decomposition of organic groups. This mass loss of organic components is equal to 1.25 mmol per g of catalyst. Furthermore, the DTG curve shows that the decomposition of the organic structure mainly occurred at 520 °C. Analysis of these diagrams strongly proposed that the phthalocyanine structure was stable and no further weight loss occurs below 400 °C. Therefore, high thermal stability of the

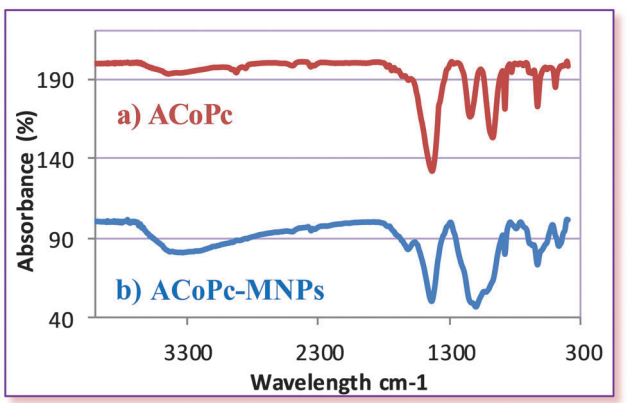

Fig. 3 FT-IR spectra of (a) ACoPc and (b) ACoPc-MNPs.

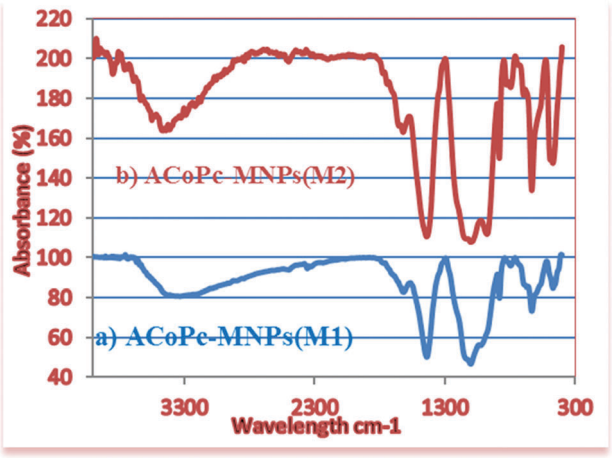

Fig. 4 FT-IR spectra for comparison of the synthesized catalyst by two methods. (a) Synthesis of the catalyst by a one-pot process by refluxing Fe_3O_4@SiO_2, ClMNPs and ACoPc (method 1); (b) synthesis of the catalyst in two steps (method 2).

catalyst indicated covalent chemical bonds between amino phthalocyanine and the support (Fig. 5).

The X-ray diffraction patterns of MNPs, MNPs@SiO_2 and ACoPc-MNPs are shown in Fig. 6.

The XRD data of the synthesized magnetic nanoparticles show diffraction peaks at 2θ = 30.4°, 35.7°, 43.3°, 53.9°, 57.3° and 63.0°, indicating that the Fe_3O_4 particles in the nanoparticles were pure with a cubic spinel structure. An amorphous silica phase in the shell of the silica-coated Fe_3O_4 nanoparticles (Fe_3O_4@SiO_2) shows broad diffraction peaks from 2θ = 20° to 27° as indicated in Fig. 6b.

Finally, the addition of Co phthalocyanine to MNPs@SiO_2 gave rise to the peaks at 17.3°, 18.5°, 20.1°, 23.5°, 28.2°, 29.3°, 32.8°, 34.4°, 35.4°, 43°, 48°, 57.3°, and 62.9° (Fig. 6c). As indicated in Fig. 6b and c, the peak positions of ACoPc-MNPs

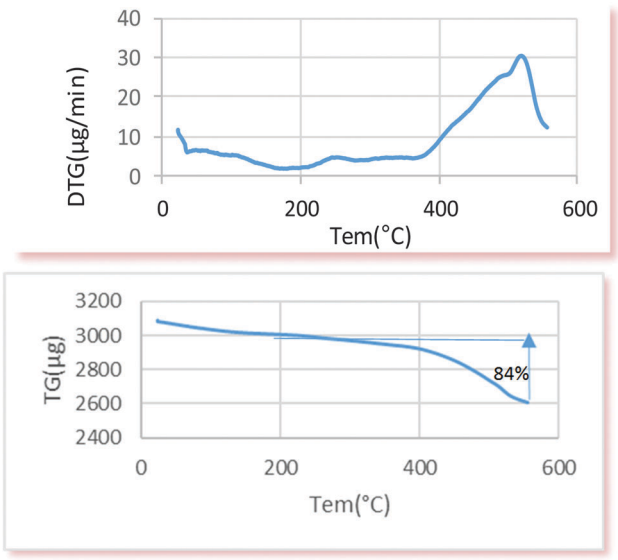

Fig. 5 TGA and DTG of ACoPc-MNPs.

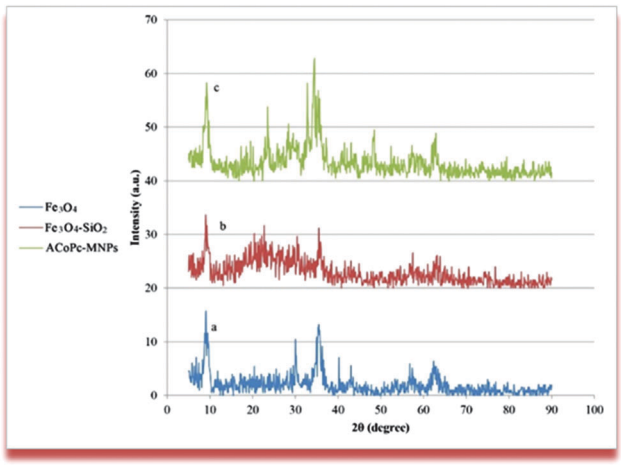

Fig. 6 XRD diffraction pattern of (a) MNPs, (b) Fe_3O_4@SiO_2 and (c) ACoPc-MNPs.

and Fe_3O_4@SiO_2 did not change because the coating of the ACoPc layer does not change the structure of the Fe_3O_4@SiO_2 nanoparticles.[21]

The components of the ACoPc-MNPs were analyzed, by using an energy dispersive spectrometer (EDS), as indicated in Fig. 7. The EDX spectrum shows the presence of Co, Si, O, N and Fe signals, and no other impurities are found (Fig. 7).

XRF analysis of the catalyst showed Co loading in ACoPc-MNPs. Co content was determined to be about 2.29 w/w% in the catalyst. The specific surface area of the catalyst was calculated from adsorption isotherms using the standard BET equation. The Brunauer–Emmett–Teller (BET) surface was calculated to be 12.49 $m^2\ g^{-1}$.

SEM and TEM were used to show the morphology and size of the catalyst (Fig. 8a and b). These images indicated that the catalyst was approximately 50 nm in size (Fig. 8).

The atomic configuration and topography of the surface of the catalyst were determined by atomic force microscopy (AFM) (Fig. 9).

The magnetic properties of MNPs@SiO_2 and ACoPc-MNPs were characterized by VSM at room temperature, as indicated in Fig. 10a and b. The two measured samples display a superparamagnetic behavior. The saturation magnetization value of

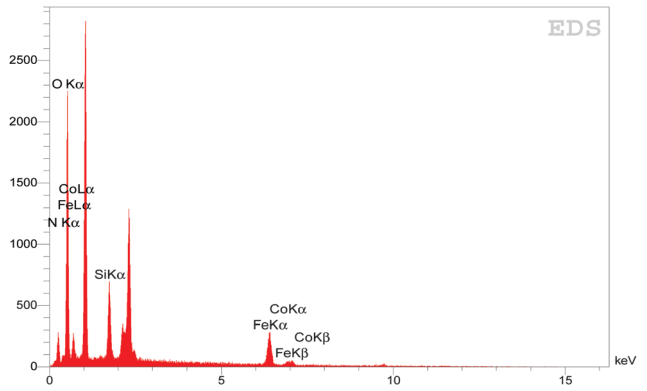

Fig. 7 EDX spectrum of ACoPc-MNPs.

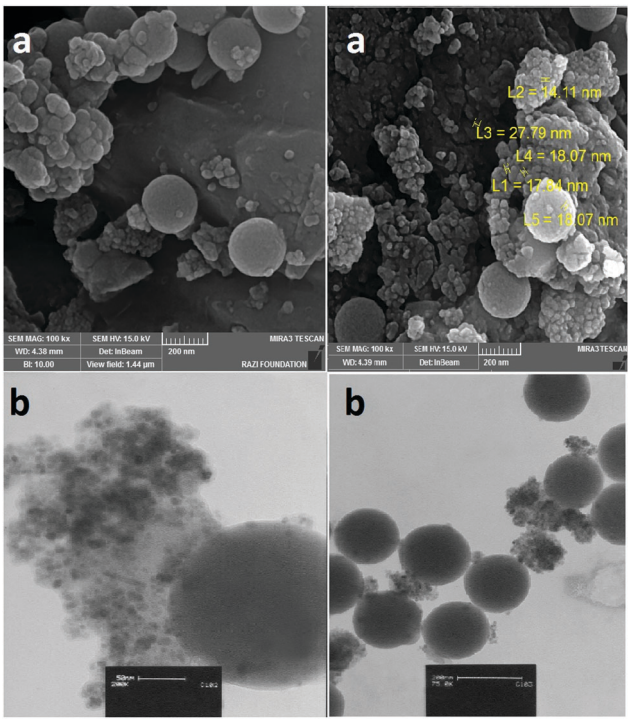

Fig. 8 SEM (a) and TEM (b) image of the ACoPc-MNPs.

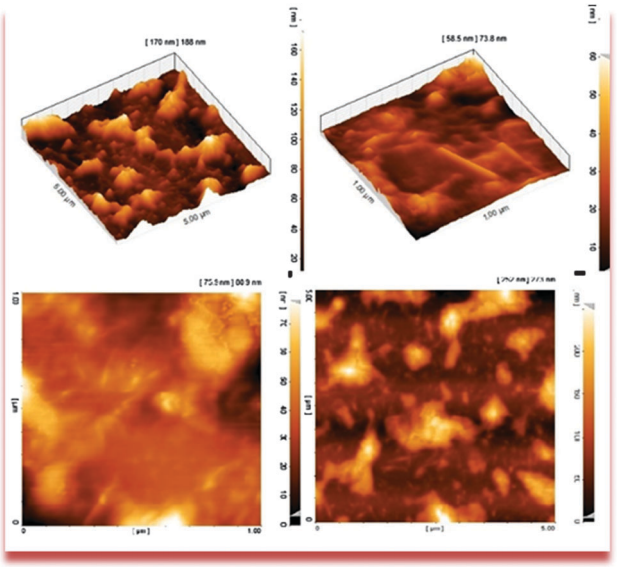

Fig. 9 AFM image of the ACoPc-MNPs.

the ACoPc-MNPs is about 8.7 emug^{-1} which is smaller than that of MNPs@SiO_2 with 25 emug^{-1}. This result confirms that the magnetite nanoparticles were coated with a non-magnetic Co phthalocyanine tag. But, the magnetization value is sufficient for common magnetic separation.

2.2. Catalyst test

The prepared magnetic nanoparticle-supported Co phthalocyanine groups have been applied as catalysts in the synthesis

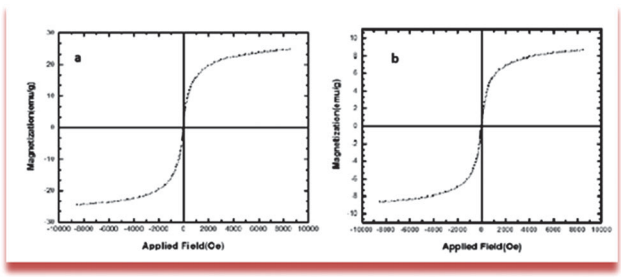

Fig. 10 The vibrating sample magnetometry (VSM) of (a) Fe_3O_4@SiO_2 and (b) the catalyst.

of tetrahydrobenzo[*b*]pyran derivatives through the reaction of malononitrile, aromatic aldehydes, and dimedone. For this purpose, the reaction of 2,5-dimethoxybenzaldehyde, malononitrile, and dimedone as a simple model reaction was probed to establish the feasibility of the strategy and optimize the reaction conditions (Scheme 4).

In order to optimize the reaction conditions and obtain the best catalytic activity, the reaction of 2,5-dimethoxybenzaldehyde (1 mmol), malononitrile (1 mmol), and dimedone (1 mmol) was used as a model, and was conducted under different reaction conditions by varying the reaction parameters such as solvent, temperature and amount of catalyst. The effect of catalyst amount was firstly investigated and different quantities of the catalyst ranging from 0.02 to 0.5 g were tested.

Thus, the best yield was found in the presence of just 0.02 g of ACoPc-MNPs (Table 1, entry 3), and the use of higher amounts of the catalyst (0.05, 0.1, 0.2 g) did not improve the result to an appreciable extent (Table 1, entries 3–11). Moreover, the model reaction was carried out in several solvents such as EtOH, H_2O, CH_3CN, CH_2Cl_2, and EtOAc, as well as in solvent-free conditions to investigate the efficiency of the catalyst (Table 2). As can be seen, the best yield was obtained when the reaction was performed under solvent free conditions (Table 2, entry 1).

The reaction was efficiently performed using 0.02 g of the nanocatalyst at room temperature under solvent free conditions to give the desired product in high yield within a short reaction time.

One-pot synthesis of tetrahydrobenzo[*b*]pyran from the reaction of various aldehydes with malononitrile and dimedone in the presence of ACoPc-MNPs was investigated (Table 3). In all cases, the three-component reaction proceeded rapidly to give the corresponding tetrahydrobenzo[*b*]pyran derivatives in moderate to good yields.

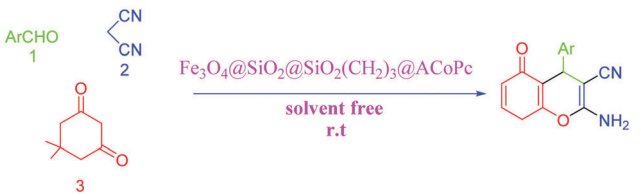

Scheme 4 ACoPc-MNP catalyzed synthesis of tetrahydrobenzo[*b*]pyran derivatives.

Table 1 Effect of different amounts of the catalyst and temperature on the reaction of 2,5-dimethoxybenzaldehyde, malononitrile, and dimedone under solvent free conditions[a]

Entry	Amount of the catalyst (g)	Reaction temperature (°C)	Reaction time (min)	Isolated yield (%)
1	—	r.t.	60	40
2	—	100	60	50
3	0.02	r.t.	15	93
4	0.02	75	15	93
5	0.02	100	15	93
6	0.05	r.t.	15	93
7	0.05	100	15	93
8	0.1	r.t.	15	93
9	0.1	100	15	93
10	0.2	r.t.	20	92
11	0.5	r.t.	20	92

[a] Reaction conditions: 2,5-dimethoxybenzaldehyde (1 mmol), malononitrile (1 mmol), and dimedone (1 mmol) under solvent free conditions.

Table 2 Effect of different solvents on the catalytic activity of ACoPc-MNPs in the synthesis of tetrahydrobenzo[*b*]pyran derivatives[a]

Entry	Solvent	Reaction time (min)	Yield (%)
1	Solvent-free	15	93
2	H_2O	45	40
3	C_2H_5OH	20	92
4	CH_3CN	20	92
5	CH_3CO_2Et	30	80
6	CH_2Cl_2	30	85

[a] Reaction conditions: 2,5-dimethoxybenzaldehyde (1 mmol), malononitrile (1 mmol), dimedone (1 mmol), and solvent (3 mL) at room temperature.

Aromatic aldehydes carrying both electron-withdrawing and electron-donating groups (*ortho*-, *meta*-, and *para*-substituted) participated well in this reaction to give the corresponding products in good to excellent yields and high purity (Table 3).

The recovery and reusability of the catalyst is very important for commercial and industrial applications. Thus, the possibility of recycling the catalyst was examined using the model reaction under optimized conditions. After completion of the reaction, the mixture was diluted with acetonitrile and the catalyst was easily and rapidly separated from the product with the aid of an external magnet and decantation of the reaction solution. The remaining magnetic nanocatalyst was further washed with ethanol to remove the residual product and dried in air. Then, the reaction vessel was charged with fresh substrate and subjected to the next reaction.

The recycled catalyst could be reused four times with a little loss of its initial catalytic activity (Fig. 11).

To compare the efficacy of the ACoPc-MNP catalyst with that of amino phthalocyanine and Fe_3O_4@SiO_2 for the synthesis of 2-amino-4-(4-chlorophenyl)-5-oxo-5,8-dihydro-4*H*-chromene-3-carbonitrile, we have presented the results obtained with the three mentioned catalysts in the condensation reaction of 4-chlorobenzaldehyde, dimedone and malononitrile in Table 4. As shown in Table 4, the ACoPc-MNP catalyst uniquely enhanced the synthesis of the desired product in different terms (reaction time and isolated yield).

Table 3 Synthesis of tetrahydrobenzo[*b*]pyran derivatives using aldehyde (1 mmol), malononitrile (1 mmol), and dimedone (1 mmol) in the presence of ACoPc-MNPs as a catalyst under solvent free conditions at room temperature

Entry	Aldehyde	Time (min)	Yield (%)	M.p (°C), [lit][ref.]
1	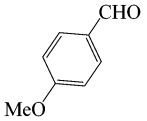	15	93	200–202 [122–12][22]
2	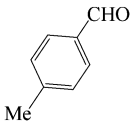	15	93	216–218 [209–211][23]
3	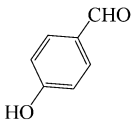	20	92	210–212 [214–215][23]
4	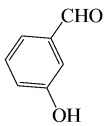	25	91	226–228 [236–238][22]
5	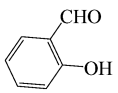	30	90	247–249[dec] (new)
6	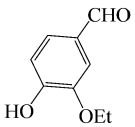	18	92	218–220 (new)
7	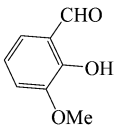	25	90	181–183 (new)
8	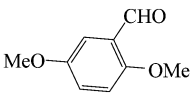	15	93	181–183 (new)
9	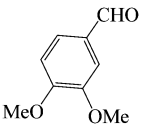	15	93	164–166 [170–173][24]
10	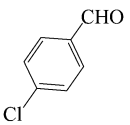	12	95	206–208 [207–209][22]
11	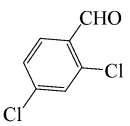	15	95	218–220 [180–182][22]
12	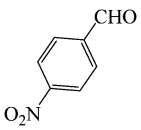	8	97	157–159 [175–176][23]
13	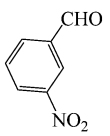	10	96	214–216 [208–211][22]

Table 3 (*continued*)

Entry	Aldehyde	Time (min)	Yield (%)	M.p (°C), [lit][ref.]
14	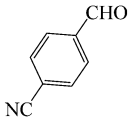	10	96	229–231 [220–225][24]
15	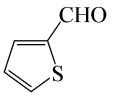	25	90	223–225 [216][24]
16	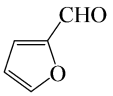	25	90	222–224 [218–220][23]

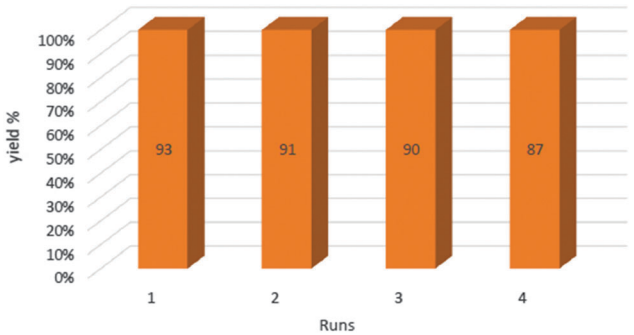

Fig. 11 The catalytic activity of ACoPc-MNPs in four cycles for the synthesis of 2-amino-4-aryl-5-oxo-4*H*,5*H*-pyrano[3,2-*c*]chromene-3-carbonitrile derivatives.

Table 4 Comparison of the results of the condensation reaction of 4-chlorobenzaldehyde, dimedone and malononitrile catalyzed by ACoPc-MNPs with the results when using amino phthalocyanine and Fe_3O_4@SiO_2 as catalysts

Catalyst[a]	Time (min)	Yield (%)
Fe_3O_4@SiO_2	40	30
ACoPc	30	50
ACoPc-MNPs	12	95

[a] Reaction conditions: 4-chlorobenzaldehyde (1 mmol), malononitrile (1 mmol), dimedone (1 mmol), and catalyst (0.02 g), under solvent free conditions at room temperature.

3. Conclusions

In summary, a novel nanomagnetically separable system in which Co phthalocyanine was chemically anchored to the nanomagnetite core was prepared and was found to be an efficient magnetically heterogeneous catalyst for the one-pot multicomponent synthesis of tetrahydrobenzo[*b*]pyran derivatives. We have shown that the advantages of the present method are (a) easy and simple work-up, (b) short reaction times, (c) mild reaction conditions, (d) room temperature of the reaction, (e) excellent yields, and (f) ease of separation of the catalyst using an external magnet. Moreover, the catalyst used is easily recovered by applying an external magnetic field and reused without any noticeable loss of activity at least 4 times. Further studies for systematic and knowledge-based development of ACoPc-MNPs are going on in our research group.

4. Experimental

4.1. Chemicals and apparatus

The materials were purchased from Merck and Fluka and were used without any additional purification. All reactions were monitored by thin layer chromatography (TLC) on gel F254 plates. Spectra (^{1}H NMR 400 MHz and ^{13}C NMR 100 MHz) were recorded in pure deuterated DMSO with tetramethylsilane (TMS) as the internal standard. The synthesized catalyst was fully characterized by FT-IR, XRD, SEM, TEM, AFM, TGA, VSM, XRF and elemental analysis.

X-ray diffraction (XRD) patterns of all catalysts were recorded on an APD 2000 (Italy) diffractometer with Cu Kα radiation (k = 0.1542 nm) operating at 50 kV and 20 mA in a 2 h range of 10–70° with step size 0.01° and time step 1.0 s to assess the crystallinity of the catalyst.

The vanadium concentration of the prepared catalysts was determined by XRF analysis (ARL8410). Fourier transform-infrared spectra of the samples were recorded on a Perkin-Elmer 17259 FT-IR spectrometer using KBr disks. Thermogravimetric analyses of catalysts were performed using a Perkin-Elmer TGA system. The weight loss between 200 and 600 °C was determined. Semi-quantitative EDX (Röntec, Quantax/QX2) analysis was used for the characterization of element concentration and vanadium distribution within the prepared catalysts. The SEM analyses were done using a TESCAN/MIRA SEM with the maximum acceleration voltage of the primary electrons between 10 and 15 kV. Transmission electron microscope (TEM) measurements were carried out on a Philips CM10 analyzer.

The magnetic measurements were carried out using a vibrating sample magnetometer (magnetite daneshpazhohan kashan/MDKB). The AFM images were obtained in ambient air using a dual scope (Cme/C26) in the constant-force mode at various scan rates.

4.2. General procedure for the synthesis of magnetite nanoparticles[25]

$FeCl_3{\cdot}6H_2O$ (9.72 g, 0.036 mol) was added to an aqueous solution of HCl 3% (v/v) and stirred for 10 min with a mechanical stirrer (mixture 1).

Na_2SO_3 (2.52 g, 0.0199 mol) was dissolved in 20 mL of deionized water until the salt was dissolved completely (mixture 2).

Mixture 2 was added dropwise to mixture 1 in 2 minutes to obtain a red solution; then, the mixture was stirred for ten minutes to obtain a yellow solution (mixture 3).

Then, 85 mL of ammonia was dissolved in 800 mL of deionized water. The resulting solution was added quickly into reaction mixture 3 in one portion to obtain a black solution. The catalyst was removed from the solution by using a magnet. The black precipitate was washed with double distilled water (seven times) and ethanol (three times) and dried in air.

4.3. Preparation of the Fe_3O_4@SiO_2 core–shell[26]

The synthesized Fe_3O_4 (2 g) were suspended in distilled water (40 mL) and sonicated for 20 min. Ethanol (16 mL), ammonia (5 mL), and tetraethyl orthosilicate (7 mL) were, respectively, added into the suspension, and continuously reacted for 12 h under stirring at room temperature. The iron oxide nanoparticles with a thin layer of silica (Fe_3O_4@SiO_2) were separated by using an external magnet, washed three times with ethanol and water, and dried under vacuum.

4.4. General procedure for the synthesis of ACoPc[27]

Ammonium molybdate (0.01 mg) was added to a solution of 3-nitrophthalic anhydride (1.93 g, 10 mmol), urea (3.0 g, 50 mmol), and $CoSO_4{\cdot}7H_2O$ (0.47 mg, 2.6 mmol) in nitrobenzene (15 mL). The mixture was stirred under N_2 at 200 °C. After 4 h, the reaction mixture was cooled and diluted with toluene (80 mL). The resulting purple precipitate was collected by centrifugation. The solid was washed with toluene, water, MeOH/ether (1 : 9), and EtOAc/hexane (2 : 1), and dried to afford a dark green solid (2.56 g, 99%). After that, sodium sulfide nonahydrate (7.4 g, 30.9 mmol) was added to tetranitro cobalt phthalocyanine (1.95 g, 2.57 mmol) in DMF (50 mL) and stirred at 70 °C for 4 h. After completion of the reaction, the mixture was cooled and collected by centrifugation. The product was washed by addition of methanol/ether (1 : 9) and methanol and washed two times with ethanol followed by centrifugation. The mixture was dried to obtain a green solid.

4.5. Preparation of ACoPc-MNPs

Fe_3O_4@SiO_2 (1.55 g), ACoPc (1.88 g) and CPTMS (7.4 g) were suspended in dried toluene and refluxed for 24 h under stirring at 110 °C. The product was separated by means of an external magnet, washed three times with toluene and dried in air to obtain a brown solid.

4.6. General procedure for the synthesis of tetrahydrobenzo[*b*]pyran derivatives

A solution of dimedone (0.066 g, 1 mmol), aromatic aldehydes (1 mmol), malononitrile (0.14 g, 1 mmol) and ACoPc-MNPs (0.02 g) was stirred at room temperature for the required time (Table 2). After completion of the reaction, as monitored by TLC, ethanol was added to the reaction mixture, and the catalyst was easily collected by means of a magnet to be reused in subsequent reactions. The obtained products were recrystallized in ethanol and characterized by ^{1}H NMR, IR and ^{13}C NMR.

4.7. Some selected spectral data of the new products

2-Amino-4-(2-hydroxyphenyl)-7,7-dimethyl-5-oxo-5,6,7,8-tetrahydro-4*H*-chromene-3-carbonitrile (Table 3, entry 5). Yellow solid; M.p: 247–249 °C; yield: 92%; IR (KBr): ν 3439, 3386, 2955, 2207, 1659, 1627, 1383 cm^{-1}; ^{1}H NMR (400 MHz, DMSO-d_6): δ_{ppm} 0.96 (s, 3H, –CH_3), 1.04 (s, 3H, –CH_3), 2.15 (d, 2H, J = 8.0 Hz, –CH_2), 2.28 (d, 2H, J = 8.2 Hz, –CH_2), 2.53 (s, 1H, –OH), 4.22 (s, 1H, –CH aliphatic), 7.13 (t, 1H, J = 6.2 Hz, ArH), 7.17 (s, 2H, –NH_2), 7.27 (d, 2H, J = 8.0 Hz, ArH), 7.36 (t, 1H, J = 7.6 Hz, ArH); ^{13}C NMR (100 MHz, DMSO-d_6): δ_{ppm} 26.8, 28.2, 31.8, 35.3, 49.9, 57.6, 112.0, 119.4, 125.9, 126.6, 127.0, 130.3, 132.9, 147.2, 158.4, 158.5, 195.7.

2-Amino-4-(3-ethoxy-4-hydroxyphenyl)-7,7-dimethyl-5-oxo-5,6,7,8-tetrahydro-4*H*-chromene-3-carbonitrile (Table 3, entry 6). White solid; M.p: 218–220 °C; yield: 95%; IR (KBr): ν 3473, 3382, 3354, 3215, 2195, 1687, 1604, 1372 cm^{-1}; ^{1}H NMR (300 MHz, DMSO-d_6): δ_{ppm} 1.02 (s, 6H, –CH_3), 2.12 (d, 2H, J = 7.1 Hz, –CH_2), 2.27 (d, 2H, J = 9.9 Hz, –CH_2), 2.51 (t, 3H, J = 5.0 Hz, –CH_3), 3.34 (q, 2H, J = 8.0 Hz, –CH_2), 4.28 (s, 2H, –CH aliphatic and –OH), 5.17 (s, 2H, –NH_2), 7.15 (s, 1H, ArH), 7.36 (d, 1H, J = 5.4 Hz, ArH), 7.75 (d, 1H, J = 5.6 Hz, ArH); ^{13}C NMR (75 MHz, DMSO-d_6): δ_{ppm} 27.0, 28.3, 31.9, 35.8, 49.9, 57.1, 109.5, 111.7, 118.8, 128.4, 132.5, 150.3, 158.5, 163.1, 195.8.

2-Amino-4-(2-hydroxy-3-methoxyphenyl)-7,7-dimethyl-5-oxo-5,6,7,8-tetrahydro-4*H*-chromene-3-carbonitrile (Table 3, entry 7). Orange solid; M.p: 181–183 °C; yield: 92%; IR (KBr): ν 3562, 3391, 3348, 2954, 2290, 1590, 1482 cm^{-1}; ^{1}H NMR (400 MHz, DMSO-d_6): δ_{ppm} 3.12 (s, 3H, –CH_3), 3.40 (s, 3H, –CH_3), 3.47 (s, 3H, –CH_3), 3.56 (s, 2H, –NH_2), 3.66 (s, 1H, –OH), 3.79 (d, 2H, J = 4.4 Hz, –CH_2), 3.90 (d, 2H, J = 4.0 Hz, –CH_2), 5.18 (s, 1H, –CH aliphatic), 6.53 (t, 1H, J = 7.8 Hz, ArH), 6.73 (d, 1H, J = 8.4 Hz, ArH), 6.84 (d, 1H, J = 4.8 Hz, ArH); ^{13}C NMR (100 MHz, DMSO-d_6): δ_{ppm} 27.9, 43.0, 55.3, 60.3, 61.9, 62.0, 72.7, 123.3, 138.3, 147.9, 150.9, 158.5, 164.4, 166.5, 168.5, 182.1, 183.2, 183.3, 196.1.

2-Amino-4-(2,5-dimethoxyphenyl)-7,7-dimethyl-5-oxo-5,6,7,8-tetrahydro-4*H*-chromene-3-carbonitrile (Table 3, entry 8). Cream solid; M.p: 181–183 °C; yield: 95%; IR (KBr): ν 3391, 3334, 3216, 2951, 2193, 1682, 1650, 1499, 1374 cm^{-1}; ^{1}H NMR (300 MHz, DMSO-d_6): δ_{ppm} 1.03 (s, 6H, –CH_3), 2.08 (d, 2H, J = 7.2 Hz, –CH_2), 2.27 (d, 2H, J = 7.1 Hz, –CH_2), 3.69 (s, 6H, –CH_3), 4.42 (s, 1H, –CH aliphatic), 5.17 (s, 2H, –NH_2), 6.50 (s, 1H, ArH), 6.73 (d, 1H, J = 5.8 Hz, ArH), 6.89 (d, 1H, J = 6.0 Hz, ArH); ^{13}C NMR (75 MHz, DMSO-d_6): δ_{ppm} 26.5, 28.7, 31.8, 50.0, 55.2, 56.3, 57.2, 111.5, 111.8, 112.6, 114.8, 119.8, 133.5, 151.0, 153.1, 158.9, 163.2, 195.6.

Acknowledgements

We thank Bu-Ali Sina University and Iran National Science Foundation (INSF) for financial support (The Grant of Allameh Tabataba 'i's Award, Grant Number: BN093) to our research group.

Notes and references

1 See reviews: (*a*) B. Karimi, F. Mansouri and H. M. Mirzaei, *ChemCatChem*, 2015, **7**, 1736; (*b*) T. Cheng, D. Zhang, H. Li and G. Liu, *Green Chem.*, 2014, **16**, 3401; (*c*) M. B. Gawande, R. Luque and R. Zboril, *ChemCatChem*, 2014, **6**, 3312; (*d*) D. Zhang, C. Zhou, Z. Sun, L. Wu, C. Tunga and T. Zhang, *Nanoscale*, 2012, **4**, 6244.

2 H. Uchida, P. Y. Reddy, S. Nakamura and T. Toru, *J. Org. Chem.*, 2003, **68**, 8736.

3 (*a*) S. L. Jain, J. K. Joseph, S. Singhal and B. Sain, *J. Mol. Catal. A: Chem.*, 2007, **268**, 134; (*b*) V. B. Sharma, S. L. Jain and B. Sain, *Tetrahedron Lett.*, 2003, **44**, 383; (*c*) C. Perollier

and A. B. Sorokin, *Chem. Commun.*, 2002, 1548–1549; (*d*) A. B. Sorokin and A. Tuel, *New J. Chem.*, 1999, **23**, 473; (*e*) R. Naik, P. Joshi and R. K. Deshpande, *J. Mol. Catal. A: Chem.*, 2005, **238**, 46; (*f*) B. Meunier and A. B. Sorokin, *Acc. Chem. Res.*, 1997, **30**, 470; (*g*) M. Alvaro, E. Carbonell, M. Espla and H. Carcia, *Appl. Catal., B*, 2005, **57**, 37; (*h*) S. Jain and B. Sain, *J. Mol. Catal. A: Chem.*, 2001, **176**, 101; (*i*) N. Grootboom and T. Nyokong, *J. Mol. Catal. A: Chem.*, 2002, **179**, 113.

4 Z. Bao, A. J. Loving and A. Dodabalapur, *Adv. Mater.*, 1997, **9**, 42.

5 (*a*) G. Guillaud, J. Simon and J. P. Germain, *Coord. Chem. Rev.*, 1998, **180**, 1433; (*b*) N. B. McKeown, *Chem. Ind.*, 1992, 92; (*c*) A. J. Duro, G. de la Torre, J. Barber, J. L. Serrano and T. Torres, *Chem. Mater.*, 1996, **8**, 1061; (*d*) G. J. Clarkson, N. B. McKeown and K. E. Treacher, *J. Chem. Soc., Perkin Trans. 1*, 1995, 1817.

6 C. G. Claessens, W. J. Blau, M. Cook, M. Hanack, R. J. M. Nolte, T. Torres and D. Wohrle, *Monatsh. Chem.*, 2001, **132**, 3.

7 (*a*) G. de la Torre, P. Vasquez and F. Agullo-Lopez, *Adv. Mater.*, 1997, **9**, 265; (*b*) G. de la Torre, P. Vaquez, F. Agullo-Lopez and T. Torres, *J. Mater. Chem.*, 1998, **8**, 1671.

8 (*a*) H. Ali and J. E. van Lier, *Chem. Rev.*, 1999, **99**, 2379; (*b*) K. Katrin, A. Nihal, C. Tracy, B. David and M. Hasan, *Cancer Res.*, 2000, **60**, 5984; (*c*) D. Phillips, *Pure Appl. Chem.*, 1995, **67**, 117; (*d*) R. Bonnett, *Chem. Soc. Rev.*, 1995, **24**, 19; (*e*) S. B. Brown and T. G. Truscott, *Chem. Br.*, 1993, **29**, 955; (*f*) C. M. Allen, W. M. Sharman and J. E. van Lier, *J. Porphyrins Phthalocyanines*, 2001, **5**, 1.

9 F. Zhao, F. Harnisch, U. Schroder, F. Scholz, P. Bogdanoff and I. Herrmann, *Electrochem. Commun.*, 2005, **7**, 1405.

10 S. Erkan, A thesis submitted to the graduate school of natural and applied sciences of Middle East technical university, 2005, p. 48.

11 (*a*) A. Kempa and J Dobrowlski, *Can. J. Chem.*, 1988, 2553; (*b*) Y. H. Tse, C. C. Leznoff and A. B. P Lever, *Inorg. Chem.*, 1991, **30**, 4453; (*c*) M. Hanack and J. Osio-Barcina, *Synthesis*, 1992, 211.

12 F. Ahangaran, A. Hassanzadehand and S. Nouri, *Int. Nano Lett.*, 2013, **3**, 23.

13 S. A. Borisenkova, E. G. Girenko, B. G. Gherassimov, L. M. Mazyarkina, V. P. Erofeeva, V. M. Derkacheva, O. L. Kaliya and E. A. Lukyanets, *J. Porphyrins Phthalocyanines*, 1999, **3**, 210.

14 (*a*) M. J. Climent, A. Corma and S. Iborra, *RSC Adv.*, 2012, **2**, 16; (*b*) J. Yu, F. Shi and L.-Z. Gong, *Acc. Chem. Res.*, 2011, **44**, 1156.

15 (*a*) W. O. Foye, *Prinicipi di Chimica Farmaceutica Piccin*, adova, Italy, 1991, p. 416; (*b*) L. L. Andreani and E. Lapi, *Boll. Chim. Farm.*, 1960, **99**, 583; (*c*) L. Bonsignore, G. Loy, D. Secci and A. Calignano, *Eur. J. Med. Chem.*, 1993, **28**, 517.

16 See our reviews: (*a*) P. Salehi, M. A. Zolfigol, F. Shirini and M. Baghbanzadeh, *Curr. Org. Chem.*, 2006, **10**, 2171; (*b*) F. Shirini, M. A. Zolfigol, P. Salehi and M. Abedini, *Curr. Org. Chem.*, 2008, **12**, 183; (*c*) M. Daraei, M. A. Zolfigol, F. Derakhshan-Panah, M. Shiri, H. G. Kruger and M. Mokhlesi, *J. Iran. Chem. Soc.*, 2015, **12**, 855; (*d*) D. Azarifar, S. M. Khatami, M. A. Zolfigol and R. Nejat-Yami, *J. Iran. Chem. Soc.*, 2014, **11**, 1223; (*e*) M. Safaiee, M. A. Zolfigol, M. Tavasoli and M. Mokhlesi, *J. Iran. Chem. Soc.*, 2014, **11**, 1593; (*f*) M. A. Zolfigol, R. Ayazi and S. Baghery, *RSC Adv.*, 2015, **5**, 71942; (*g*) M. A. Zolfigol, A. Khazaei, M. Safaiee, M. Mokhlesi, R. Rostamian, M. Bagheri, M. Shiri and H. G. Kruger, *J. Mol. Catal. A: Chem.*, 2013, **370**, 80; (*h*) A. Khazaei, M. A. Zolfigol, M. Safaiee, M. Mokhlesi, E. Donyadari, M. Shiri and H. G. Kruger, *Catal. Commun.*, 2012, **26**, 34.

17 (*a*) T. Azadbakht, M. A. Zolfigol, R. Azadbakht, V. Khakizadeh and D. Perrin, *New J. Chem.*, 2015, **39**, 439; (*b*) M. A. Zolfigol, T. Azadbkht, V. Khakizadeh, R. Nejatyami and D. Perrin, *RSC Adv.*, 2014, **4**, 40036; (*c*) M. A. Zolfigol, V. Khakyzadeh, A. R. Moosavi-Zare, A. Rostami, A. Zare, N. Iranpoor, M. H. Beyzavie and R. Luque, *Green Chem.*, 2013, **15**, 2132; (*d*) N. Koukabi, E. Kolvari, A. Khazaei, M. A. Zolfigol, B. Shirmardi-Shaghasemi and H. R. Khavasi, *Chem. Commun.*, 2011, **47**, 9230.

18 (*a*) M. A. Zolfigol, A. R. Pourali, S. Sajjadifar and S. Farahmand, *Curr. Catal.*, 2013, **2**, 151; (*b*) M. Safaiee, M. A. Zolfigol, F. Afsharnadery and S. Baghery, *RSC Adv.*, 2015, **5**, 102340.

19 G. Mbambisa and T. Nyokong, *Polyhedron*, 2008, **27**, 2799.

20 H. Moghanian, A. Mobinikhaledi, A. G. Blackmanc and E. Sarough-Farahanib, *RSC Adv.*, 2014, **4**, 28176.

21 M. Esmaeilpour, A. R. Sardarian and J. Javidi, *Appl. Catal., A*, 2012, **445**, 359.

22 E. Mosaddegh, A. Hassankhani and G. Mansouri, *E-J. Chem.*, 2011, **8**, 529.

23 B. Boumoud, A. A. Yahiaoui and T. Boumoud, *Asian J. Biochem. Pharm. Res.*, 2012, **4**, 795.

24 S. R. Kamat, A. H Mane, S. M. Ardeand and R. S. Salunkhe, *Int. J. Pharm., Chem. Biol. Sci.*, 2014, **4**, 1012.

25 S. Qu, H. Yang, D. Ren, S. Kan, G. Zou, D. Li and M. Li, *J. Colloid Interface Sci.*, 1999, **215**, 190.

26 Y.-H. Deng, C.-C. Wang, J.-H. Hu, W.-L. Yang and S.-K. Fu, *Colloids Surf., A*, 2005, **262**, 87.

27 (*a*) M. Wyler, *US. Pat. Appl.*, 2197458, 1940 (*Chem. Abstr.*, 1940, **34**, 37564); (*b*) M. Wyler, *US. Pat. Appl.*, 2197459, 1940 (*Chem. Abstr.*, 1940, **34**, 37564); (*c*) J. Alzeer, P. J. C. Roth and N. W. Luedtke, *Chem. Commun.*, 2009, 1970.